



Heat and Mass Transfer in MHD Flow about an Inclined Porous Plate

Linah Mogirango Onyinkwa ^{a*} and Isaac Chepkwony ^a

^a Kenyatta University, Kenya.

Authors' contributions

This work was carried out in collaboration between both authors. Both authors read and approved the final manuscript.

Article Information

DOI: 10.9734/JERR/2023/v25i4906

Open Peer Review History:

This journal follows the Advanced Open Peer Review policy. Identity of the Reviewers, Editor(s) and additional Reviewers, peer review comments, different versions of the manuscript, comments of the editors, etc are available here: <https://www.sdiarticle5.com/review-history/102081>

Original Research Article

Received: 22/04/2023

Accepted: 24/06/2023

Published: 24/06/2023

ABSTRACT

In this study, we explore how mass and heat are transferred in magnetohydrodynamics (MHD) flow. MHD has several applications in Power Generation, Magnetohydrodynamic Pumps, Plasma and Fusion Research, Spacecraft Propulsion, Metal Casting and Materials Processing, Geophysics and Planetary Science. Our focus is on understanding the flow over an inclined plate positioned near a semi-infinite porous plate. To tackle this problem, we combine the laws of electromagnetism with the Navier-Stokes equations to develop a comprehensive MHD flow model. To analyse the behaviour of the flow, we transform the governing equations into a simpler, dimensionless form. Employing the Implicit finite centre difference, we obtain the numerical solutions for the equations. These solutions allow us to visualize the results through graphical representations. Our investigation delves into the effects of various parameters on the flow characteristics. Specifically, we examine the influence of the porosity parameter, magnetic strength parameter, and inclination angle. As we analyse these factors, we observe interesting trends. The velocity profiles in all directions exhibit a decreasing trend as porosity, magnetic field strength, and inclination angle increase. On the other hand, as the porosity, magnetic field strength, and surface inclination angle increase, we observe a notable augmentation in the temperature profiles.

*Corresponding author;

Keywords: Heat and mass transfer; power generation; magnetohydrodynamics (MHD) flow; velocity profiles.

NOMENCLATURE

Symbols	Meaning	Symbols	Meaning
u, v, w	Dimensional velocities in the x, y, z directions (LT^{-1})	Gr_t^1, Gr_t^2	Thermal Grashof number in the x - and y - directions respectively
T	Dimensional temperature (K)	Gr_s^1, Gr_s^2	Solutal Grashof number in the x - and y - directions respectively
C	Dimensional concentration (L^{-3})	M	Magnetic field parameter
$T_w (T_\infty)$	Temperature of the wall (free stream) (K)	k	Thermal diffusivity (L^2T^{-1})
C_w, C_∞	Concentration of the wall and free stream respectively (L^{-3})	k_*	Porosity parameter
B_0	Magnetic field strength (AL^{-1})	Sc	Schmidt number
K_0	Porosity	N_b, N_t	Brownian and thermophoretic parameters
D_B	Brownian coefficient	HMT	Heat and Mass Transfer
D_T	Thermophoretic coefficient	MF	Magnetic field
η	Similarity variable	ρ	Density of fluid (ML^{-3})
β, β^*	Coefficient of thermal and solutal expansivity	c_p	Heat capacity of the fluid ($ML^2T^{-2}K^{-1}$)
g^*	Acceleration due to gravity (LT^{-2})	σ	Electrical conductivity ($M^{-1}L^{-3}T^3A^2$)
α	Inclination angle	μ	Dynamic viscosity ($ML^{-1}T^{-1}$)
ν	Kinematic viscosity (L^2T^{-1})		

1. INTRODUCTION

Heat and mass transfer finds wide-ranging applications in both scientific and technological domains, contributing to the operations of devices and systems, heat engines, thermal diodes, and thermoelectric warmers. Additionally, heat exchangers serve as a prevalent application of heat transfer, commonly employed in refrigeration and chemical processing. Mass transfer occurs in diverse processes, including membrane filtration and adsorption. Until now, scholarly focus has not been directed towards the analysis of flow within a three-dimensional framework where the flow traverses an inclined surface, causing the flow to move against the gravitational force. This study endeavours to unravel the characteristics of such a flow occurring in a three-dimensional context [1–6].

The utilization of MHD flow on an inclined porous surface finds application in MHD generators and flow meters. This knowledge contributes to addressing societal needs, particularly in mineral exploration, which generates income for miners.

Furthermore, the study of plasma confinement holds promise in overcoming the global energy shortage, a pressing challenge faced by human society [7]. Additionally, MHD energy generation is renowned for its environmentally friendly nature, as it operates without emitting pollutants, thus significantly reducing environmental pollution. Given its wide-ranging applications in research and technology, a comprehensive understanding of heat and mass transfer in MHD systems is crucial. Hannes Alfvén (1908-1995) is widely credited for his significant contributions to the field of MHD research [8]. One of his notable predictions was that the Earth's magnetic field would induce currents in the ocean. Since then, numerous scholars have embarked on analytical studies in MHD, uncovering a plethora of applications, particularly in the realm of heat generation and natural convection phenomena. These investigations involve formulating boundary value problems, assuming steady and two-dimensional motion, along with incompressible fluid flow, while neglecting friction-induced heating. Drawing inspiration from Khan et al. [9], who investigated MHD

incompressible Couette flow induced by a spontaneously moving plate, and Shivaiah & Rao [10], who explored MHD free convective heat and mass transfer flow past a vertically accelerated porous plate, the study seeks to shed light on the relationship between magnetic parameters, skin friction, and various transport phenomena. Considering the practical implications, Onyango et al. [11] examined MHD flow between two parallel porous plates, accounting for injection and suction effects. They noted an interesting phenomenon – the velocity profile increased with higher pressure gradients, pointing to the significance of such factors in MHD systems. In one study, Nyabuto et al. [12] delved into MHD Stokes-free convection of an incompressible fluid on a vertical porous semi-infinite plate. By applying a uniform magnetic field perpendicular to the flow, they observed a fascinating outcome—increasing the Hartmann number led to a decrease in the velocity profile. Building upon these findings, the proposed research aims to explore a three-dimensional fluid flow system influenced by an externally applied magnetic field. Oke et al. [13–15] embarked on a captivating investigation centred around the impact of the Coriolis force on the motion of air over an ultra-high-speed projectile. The findings provided valuable insights into atmospheric dynamics, showcasing the significant influence of the Coriolis force on air movement.

Examining the impact of Hall current on unsteady MHD Hartmann-Couette flow, Beg et al. [16] shed light on this intriguing phenomenon. They explored the intricate dynamics and interactions within the system. Ali et al. [17] focused their attention on the influence of thermal radiation on free convective flow along a vertical surface in a medium consisting of gray gas. Their study sought to elucidate the effects and implications of thermal radiation in this particular flow scenario. Nayak et al. [18] focused on MHD flow within a channel, where one of the plates was in motion. Their study aimed to elucidate the behaviour and characteristics of this particular flow configuration. In a noteworthy study, Mburu Mbugua [19] delved into MHD flow between two parallel porous plates, with one plate in motion. Their investigation revealed a direct proportionality between the temperature profile and the suction parameter, while the velocity exhibited an inverse relationship with the suction parameter. Umamaheswar et al. [20] explored the influence of viscous dissipation on MHD flow of a viscoelastic fluid past an inclined permeable

plate. By examining the interplay between these factors, they deepened our understanding of the behaviour exhibited in such flows. In a comprehensive analysis, Hayat et al. [21] investigated the effects of cross-diffusion on forced convection heat transfer in the boundary layer flow of elastic-viscous fluids along a stretched surface in a porous medium. Their study contributed to understanding the complexities associated with this flow scenario. Investigating time-dependent MHD natural convection flow through a vertical permeable flat plate for a nanofluid with constant heat generation, Hamad et al. [22] provided valuable insights into the intricate dynamics of this complex system.

Studies conducted on MHD fluid flow [23–26] have primarily focused on examining the characteristics of the fluid in a two-dimensional flow, which may not adequately capture the behaviour observed in real-world physical systems.

MHD flow on an inclined porous surface is applied in MHD generators and flow meters. The knowledge is applied in meeting societal needs as it is used in mineral exploration which gives the miners income. Study of plasma confinement will help mankind to remove energy shortage which is a major problem in the human society. Furthermore, because MHD energy generation is pollution-free, it will considerably reduce environmental pollution. Because of its wide applicability in research and technology, understanding HMT in MHD is essential. The objective of this research is to explore the intricacies of three-dimensional fluid flow over a porous plate that is inclined at an angle relative to the direction of fluid flow, encompassing scenarios relevant to bulk systems. Investigating MHD flow on an inclined porous surface holds significant importance as it can provide valuable insights into the nature of the fluid and find practical applications in plasma studies, the petroleum industry, and engineering fields. The aim is achieved by determining the MF effects on mass transfer in MHD flow about a plate inclined at an angle past semi-infinite porous plate.

2. FORMULATION OF GOVERNING EQUATIONS

The laminar incompressible viscous flow considered in this study is a three-dimensional flow across an inclined porous plate with constant magnetic field. The flow is taken in a

magnetic field (MF) with constant MF strength. The assumptions for the flow are;

- fluid flow is incompressible and steady;
- concentration of foreign mass is low hence Dufour and Soret effects can be ignored.
- the plate is at rest and it is a non-conductor,
- the hall current is too small and there is no applied or polarization voltage, magnetic field is applied orthogonal to the plate and induced MF is negligible.

The x -axis is taken horizontally parallel to the plate along the flow, y axis is perpendicular to the semi-infinite porous plate. The MF strength that is applied perpendicularly to the semi-infinite porous plate has uniform strength B_0 . The fluid layer next to the surface is considered to take the surface properties to ascertain that the no-slip condition is maintained. The surface stretches linearly at the rate ax and the correction factor $\cos \alpha$ is included in the corresponding terms to pay for the inclination of the surface. The model consists of the continuity,

momentum, energy and mass concentration equations. The physical configuration of the flow is shown in Fig. 1.

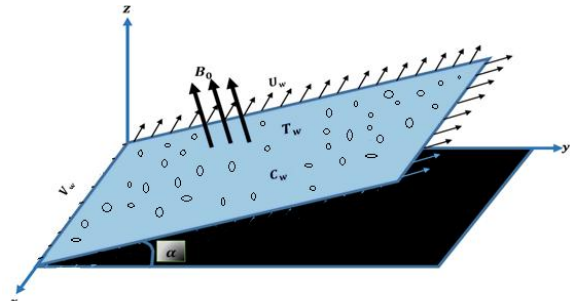


Fig. 1. Flow configuration

The boundary layer equations obtained from the Navier Stokes' equations are given as the system of five Partial Difference Equations (PDEs) consisting of one continuity equation, two momentum equations (because the flow is three-dimensional), one energy equation and one species equation. Following the ideas of [27–31], The system is as follows;

$$\left\{ \begin{array}{l} \nabla \cdot \underline{U} = 0 \quad (2.1a) \\ u \frac{\partial u}{\partial x} + v \frac{\partial u}{\partial y} + w \frac{\partial u}{\partial z} = \nu \frac{\partial^2 u}{\partial z^2} + g^*(\beta(T - T_\infty) + \beta^*(C - C_\infty)) \cos \alpha - \frac{\sigma B_0^2 \cos \alpha}{\rho} u - \frac{\nu}{K_0} u \quad (2.1b) \\ u \frac{\partial v}{\partial x} + v \frac{\partial v}{\partial y} + w \frac{\partial v}{\partial z} = \nu \frac{\partial^2 v}{\partial z^2} + g^*(\beta(T - T_\infty) + \beta^*(C - C_\infty)) \cos \alpha + \frac{\sigma B_0^2 \cos \alpha}{\rho} v - \frac{\nu}{K_0} v \quad (2.1c) \\ u \frac{\partial T}{\partial x} + v \frac{\partial T}{\partial y} + w \frac{\partial T}{\partial z} = \frac{k}{\rho c_p} \frac{\partial^2 T}{\partial z^2} + \tau \left(\frac{D_B}{\Delta C} \frac{\partial C}{\partial z} \frac{\partial T}{\partial z} + \frac{D_T}{T_\infty} \left(\frac{\partial T}{\partial z} \right)^2 \right) \quad (2.1d) \\ u \frac{\partial C}{\partial x} + v \frac{\partial C}{\partial y} + w \frac{\partial C}{\partial z} = D_B \frac{\partial^2 C}{\partial z^2} + \frac{D_T \Delta C}{T_\infty} \frac{\partial^2 T}{\partial z^2} \quad (2.1e) \end{array} \right.$$

where $\underline{U} = (u, v, w)$ and subject to the boundary layer and free stream conditions;

$$\left\{ \begin{array}{l} u = ax, \quad v = ay, \quad w = 0, \quad T = T_w, \quad C = C_w \quad \text{at } z = 0 \quad (2.2a) \\ u \rightarrow 0, \quad v \rightarrow 0, \quad T \rightarrow T_\infty, \quad C \rightarrow C_\infty \quad \text{as } z \rightarrow \infty \quad (2.2b) \end{array} \right.$$

2.1 Similarity Transformation

The first step in solving system (2.1) with the condition (2.2) is the reduction of the system to its dimensionless form. This process requires the use of the Similarity variables

$$\left\{ \begin{array}{l} \eta = z \left(\frac{a}{\nu} \right)^{\frac{1}{2}}, \quad \Theta = \frac{T - T_\infty}{T_w - T_\infty}, \quad \Phi = \frac{C - C_\infty}{C_w - C_\infty}, \quad (2.3) \\ u = axf', \quad v = ayg', \quad w = -(av)^{\frac{1}{2}}(f + g). \end{array} \right.$$

and the dimensionless form of the system of equations (3.1) becomes

$$f'''' - (f')^2 + (f + g)f'' + (Gr_t^1\Theta + Gr_s^1\Phi - Mf') \cos \alpha - k_*f' = 0, \tag{2.6a}$$

$$g'''' - (g')^2 + (f + g)g'' + (Gr_t^2\Theta + Gr_s^2\Phi - Mg') \cos \alpha - k_*g' = 0, \tag{2.6b}$$

$$\Theta'' + Pr(f + g)\Theta' + N_b\Phi'\Theta' + N_t(\Theta')^2 = 0, \tag{2.6c}$$

$$\Phi'' + \frac{N_t}{N_b}\Theta'' + Sc(f + g)\Phi' = 0. \tag{2.6d}$$

and the dimensionless form of the boundary conditions (2.2)

$$\left\{ \begin{array}{l} \text{at } \eta = 0; \quad f' = 1; \quad g' = 1; \quad f + g = 0; \quad \Theta = 1; \quad \Phi = 1 \end{array} \right. \tag{2.7a}$$

$$\left\{ \begin{array}{l} \text{as } \eta \rightarrow \infty; \quad f' = 0; \quad g' = 0; \quad \Theta = 0; \quad \Phi = 0; \end{array} \right. \tag{2.7b}$$

Where

$$\left\{ \begin{array}{l} Gr_t^1 = \frac{g^*\beta(T_w - T_\infty)}{a^2x}, \quad Gr_s^1 = \frac{g^*\beta^*(C_w - C_\infty)}{a^2x}, \quad M = \frac{\sigma B_0^2}{a\rho}, \end{array} \right. \tag{2.8a}$$

$$\left\{ \begin{array}{l} k_* = \frac{\nu}{aK_0}, \quad Sc = \frac{\nu}{D_B}, \quad Gr_t^2 = \frac{g^*\beta(T_w - T_\infty)}{a^2y}, \quad Gr_s^2 = \frac{g^*\beta^*(C_w - C_\infty)}{a^2y}, \end{array} \right. \tag{2.8b}$$

$$\left\{ \begin{array}{l} Pr = \frac{\nu\rho c_p}{k}, \quad N_b = \frac{\tau D_B \rho c_p}{k}, \quad N_t = \frac{\rho c_p \tau D_T}{kT_\infty} (T_w - T_\infty) \end{array} \right. \tag{2.8c}$$

3. NUMERICAL METHODS

The dimensionless form (2.6) and (2.8) are converted to a system of first order ordinary differential equations by setting

$$\begin{aligned} x_1 = f, \quad x_2 = f', \quad x_3 = f'', \quad x_4 = g, \quad x_5 = g', \\ x_6 = g'', \quad x_7 = \Theta, \quad x_8 = \Theta', \quad x_9 = \Phi, \quad x_{10} = \Phi', \end{aligned}$$

and we have

$$\left\{ \begin{array}{l} x'_1 = x_2, \quad x'_2 = x_3 \\ x'_3 = -(-x_2^2 + (x_1 + x_4)x_3 + (Gr_t^1 x_7 + Gr_s^1 x_9 - Mx_2) \cos \alpha - k_*x_2), \\ \quad x'_4 = x_5, \quad x'_5 = x_6 \\ x'_6 = -(-x_5^2 + (x_1 + x_4)x_6 + (Gr_t^2 x_7 + Gr_s^2 x_9 - Mx_5) \cos \alpha - k_*x_5) \\ \quad x'_7 = x_8 \\ \quad x'_8 = -(Pr(x_1 + x_4)x_8 + N_b x_8 x_{10} + N_t x_8^2), \\ \quad x'_9 = x_{10}, \quad x'_{10} = -\left(\frac{N_t}{N_b} x'_8 + Sc(x_1 + x_4)x_{10}\right) \end{array} \right. \tag{3.1}$$

with the boundary conditions

$$x_2(0) = 1, \quad x_5(0) = 1, \quad x_1(0) + x_4(0) = 0, \quad x_7(0) = 1, \quad x_9(0) = 1, \tag{3.2a}$$

$$x_2(\infty) = 0, \quad x_5(\infty) = 0, \quad x_7(\infty) = 0, \quad x_9(\infty) = 0. \tag{3.2b}$$

The coefficient of skin friction is given as

$$Re^{\frac{1}{2}} C_f = f''(0),$$

where Re is the Reynold's number.

4. RESULTS AND DISCUSSION

The Implicit centre difference scheme [32] is used to solve the system of first order ODEs (3.1) numerically and the results are displayed as graphs. The default values of the parameters used are

$$Gr_t^1 = Gr_t^2 = Gr_s^1 = Gr_s^2 = 1, \quad M = 1, \quad k_* = 1, \\ Pr = 7, \quad N_b = N_t = 1, \quad Sc = 1.$$

The Figs. (2) – (5) highlight the impact of inclination angle on the magnetohydrodynamic flow around a slanted porous plate. Both the secondary velocity and the primary velocity decrease as the inclination angle increases, as shown in Figs. (2) and (5). It is important to note that when $\alpha=0$, the surface is flat and horizontal, while it becomes inclined for $0 < \alpha < \pi/2$ and vertical at $\alpha=\pi/2$. Therefore, an increase in the inclination angle results in more conversion of kinetic energy into heat energy, leading to reduced velocities in all directions. The temperature and concentration profiles, depicted in Fig. (4) and (5), shows an increase with higher inclination angles, with the maximum temperature occurring at an inclination angle of $\pi/2$.

Figs. (6) – (9) illustrate the changes in velocities, temperature, and concentration with increasing porosity. Porosity refers to the ratio of empty spaces or pores to the volume of the plate. As porosity increases, the fluid's viscosity also increases, leading to a reduction in flow velocities, as shown in Figs. (6) and (7). Increased porosity allows molecules to settle at the plate's wall, resulting in a surge in concentration at the wall, as

depicted in Fig. (8). Heat transfer from the wall to the free stream is slowed down, enhancing the temperature profile. Thus, higher porosity levels contribute to an increased temperature profile, as shown in Fig. (9).

Figs. (10) – (13) demonstrate the effects of increasing magnetic field (MF) on the flow properties. The presence of a magnetic field generates the Lorentz force, which opposes motion and consequently reduces both primary and secondary velocities. Therefore, Figs. (10) and (11) indicate that stronger magnetic fields result in decreased flow velocities. Additionally, the resistance caused by the Lorentz force generates more heat, leading to an increase in flow temperature, as observed in Fig. (12) which shows the variation of temperature with the MF parameter. Fig. (13) displays an increase in concentration with increasing MF strength.

Table 1 shows the variation of coefficient of skin friction with increasing magnetic field, porosity and inclination angle. The table shows that the skin friction increases with increasing magnetic field, porosity and inclination angle. Increase in the MF strength increases the viscous boundary layer and thereby raising the skin friction. The increase in the porosity enhances the migration of the fluid particles towards the boundary layer and thereby gives rise to an increase in the coefficient of skin friction. Also, as the angle of inclination increases from 0° through 90° , fluid particles are more attracted to the boundary layer. Hence, the skin friction is boosted as inclination angle increases.

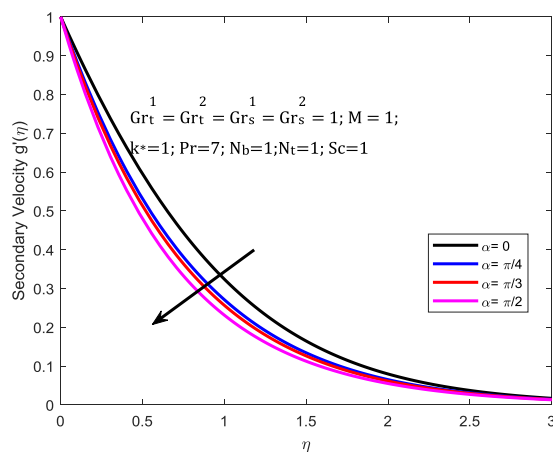


Fig. 2. Secondary velocity profile as inclination angle varies

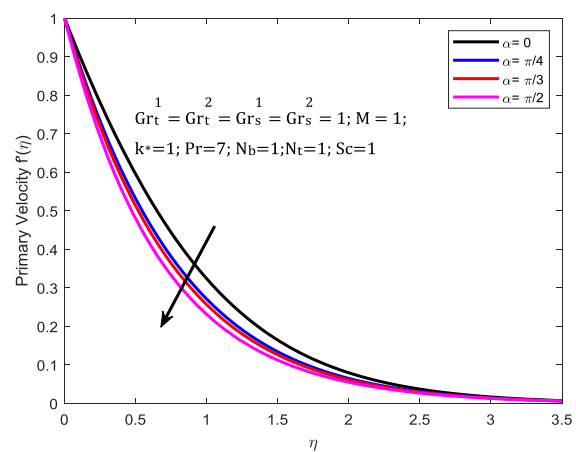


Fig. 3. Primary velocity profile as inclination angle varies

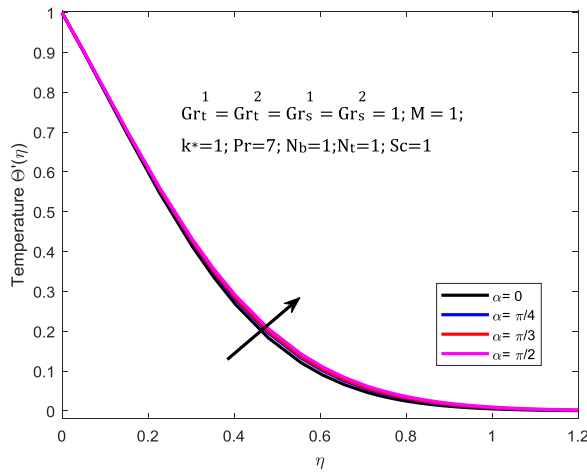


Fig. 4. Temperature profile as inclination angle varies

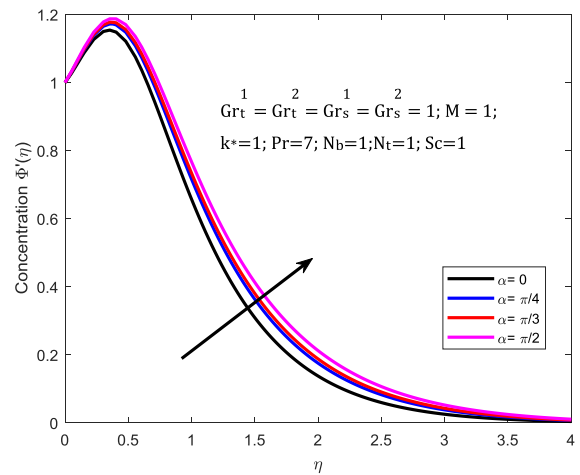


Fig. 5. Concentration profile as inclination angle varies

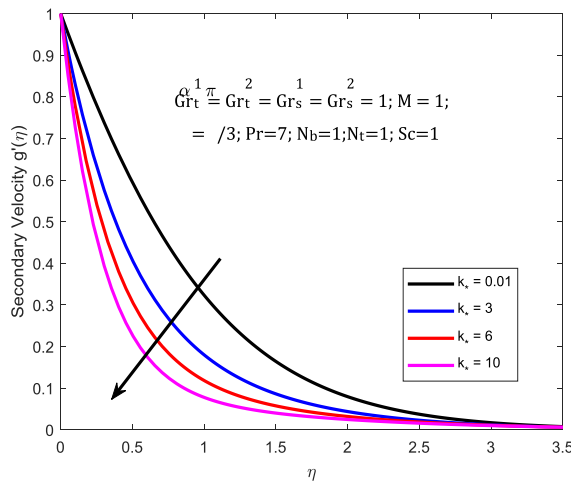


Fig. 6. Secondary velocity profile as porosity varies

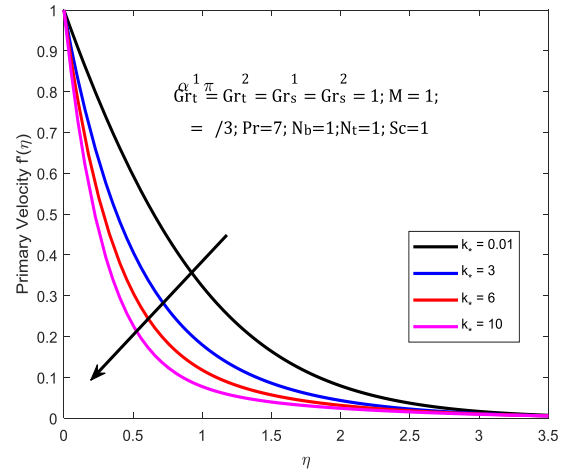


Fig. 7. Primary velocity profile as porosity varies

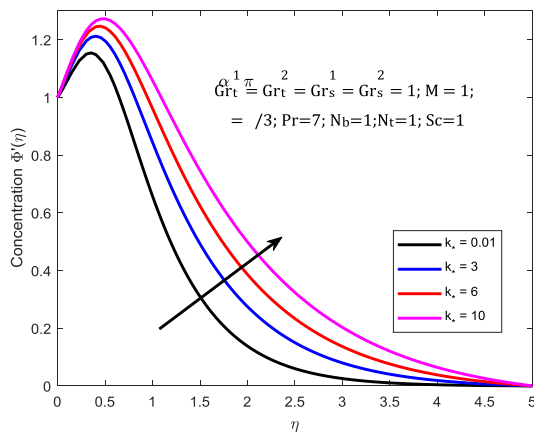


Fig. 8. Concentration profile as porosity varies

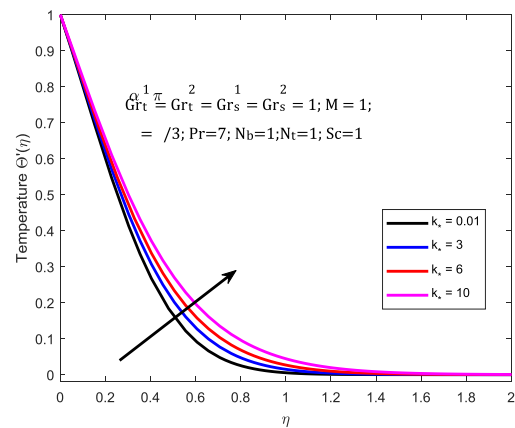


Fig. 9. Temperature profile as porosity varies

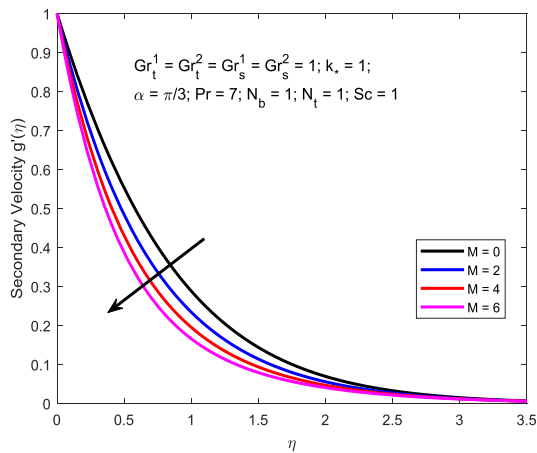


Fig. 10. Secondary velocity profile as MF parameter varies

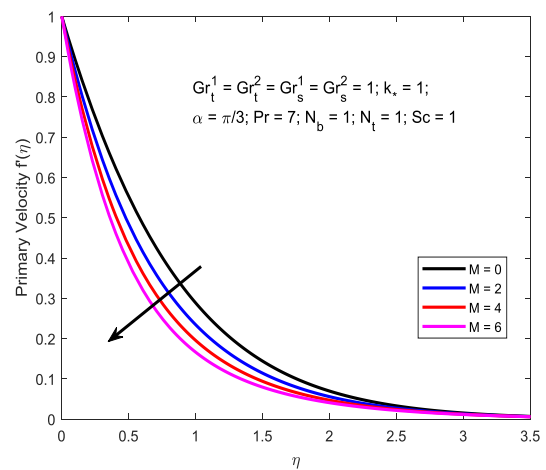


Fig. 11. Primary velocity profile as MF parameter varies

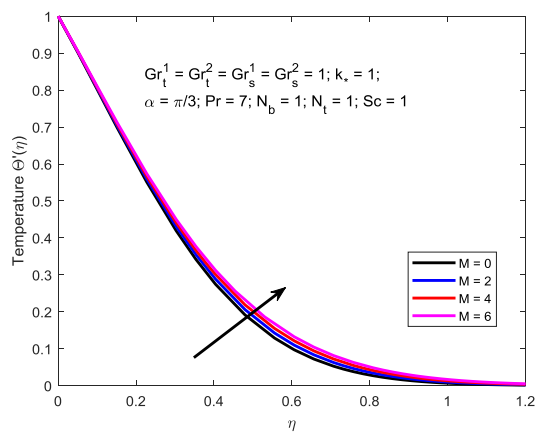


Fig. 12. Temperature profile as MF parameter varies

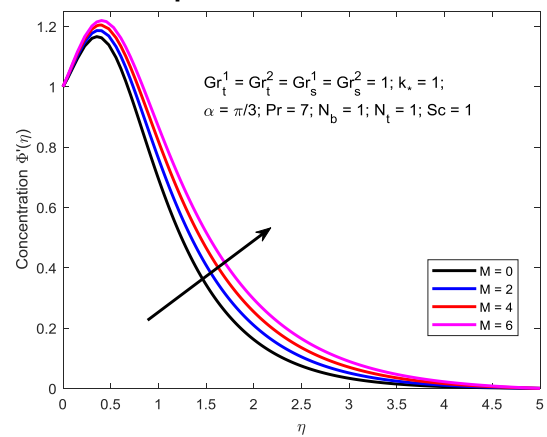


Fig. 13. Concentration profile as MF parameter varies

Table 1. Variation of coefficient of Skin Friction with magnetic field, porosity and inclination angle

M	k_*	α	Skin Friction
0.00	1.00	60°	1.1233
1.00			1.2897
2.00			1.4434
3.00			1.5865
4.00			1.7208
5.00			1.8476
1.00	0.30		1.0525
	0.90		1.2575
	1.20		1.3525
	1.50		1.4434
	1.00	0°	1.0916
		30°	1.1417
		45°	1.2037
		90°	1.5357

4. CONCLUSION

The heat and mass transfer of the magnetohydrodynamics flow of a fluid across an inclined porous plate is modelled in this study. The governing equations comes out as a system of nonlinear PDEs. Similarity variables are used to transform the PDEs into a system of ODEs which are later solved using the Finite Difference method. The effects of inclination angle and porosity on the flow about an inclined porous plate are analysed and discussed and the outcomes show that;

- Increasing inclination angles reduces both the secondary velocity and the primary velocity and increases skin friction, temperature and concentration.
- The maximum temperature profile is obtained at an inclination angle $\frac{\pi}{2}$. Increasing porosity reduces both primary and secondary velocities but increases the concentration, skin friction and temperature at the wall.
- Raising the strength of the MF reduces primary and secondary velocity and increases the flow temperature. Also, Skin friction rises with magnetic field.

COMPETING INTERESTS

Authors have declared that no competing interests exist.

REFERENCES

1. Ali B, Ahammad NA, Awan AU, Oke AS, Tag-EIDin EM, Shah FA, et al. The dynamics of water-based nanofluid subject to the nanoparticle's radius with a significant magnetic field: the case of rotating micropolar fluid. *Sustainability*. 2022; 14(17):10474.
2. Rani KS, Reddy GVR, Oke AS. Significance of Cattaneo-Christov heat flux on chemically reacting nanofluids flow past a stretching sheet with joule heating effect. *CFD Lett*. 2023;15(7):31-41.
3. Areekara S, Sabu AS, Mathew A, Oke AS. Transport phenomena in Darcy-Forchheimer flow over a rotating disk with magnetic field and multiple slip effects: modified Buongiorno nanofluid model. *Waves Random Complex Media*. 2023:1-20.
4. Oke AS. Heat and mass transfer in 3D MHD flow of EG-based ternary hybrid nanofluid over a rotating surface. *Arab J Sci Eng*. 2022;47(12):16015-31.
5. Samuel OA. Coriolis effects on air, nanofluid and Casson fluid flow over a surface with nonuniform thickness; 2022 ([doctoral dissertation]. Kenyatta University).
6. Oke AS. Theoretical analysis of modified Eyring Powell fluid flow. *J Taiwan Inst Chem Eng*. 2022;132:104152.
7. Juma BA, Oke AS, Mutuku WN, Ariwayo AG, Ouru OJ. Dynamics of Williamson fluid over an inclined surface subject to Coriolis and Lorentz forces. *J Eng Appl Sci [lett]*. 2022; 5(1):37-46.
8. Juma BA, Oke AS, Ariwayo AG, Ouru OJ. Theoretical analysis of MHD Williamson flow across a rotating inclined surface.
9. Khan I, Fakhar K, Shafie S. Magnetohydrodynamic free convection flow past an oscillating plate embedded in a porous medium. *J Phys Soc Jpn*. 2011; 80(10):104401.
10. Shivaiah S, Rao AJ. Chemical reaction effect on an unsteady MHD free convection flow past a vertical porous plate in the presence of suction or injection. *Theor Appl Mech (Belgr)*. 2012;39(2):185-208.
11. Onyango ER, Kinyanjui MN, Uppal SM. Unsteady hydromagnetic Couette flow with magnetic field lines fixed relative to the moving upper plate. *Am J Appl Math*. 2015;3(5):206-14.
12. Nyabuto R, Sigey KJ. Investigating the unsteady MHD mixed convective flow with hall effect of A viscous incompressible fluid past A vertical porous plate with heat source. *Int J Eng Sci Innov Technol*. 2015;7(2):52-62.
13. Oke AS, Fatunmbi EO, Animasaun IL, Juma BA. Exploration of ternary-hybrid nanofluid experiencing Coriolis and Lorentz forces: Case of three-dimensional flow of water conveying carbon nanotubes, graphene, and alumina nanoparticles. *Waves Random Complex Media*. 2022:1-20.
14. Oke AS, Mutuku WN, Kimathi M, Animasaun IL. Insight into the dynamics of non-Newtonian Casson fluid over a rotating non-uniform surface subject to Coriolis force. *Nonlinear Eng*. 2020;9(1):398-411.
15. Oke AS, Prasannakumara BC, Mutuku WN, Gowda RJP, Juma BA, Kumar RN, et al. Exploration of the effects of Coriolis force and thermal radiation on water-based hybrid nanofluid flow over an exponentially stretching plate. *Sci Rep*. 2022;12(1):21733.

16. Bég OA, Bakier AY, Prasad VR. Numerical study of free convection magnetohydrodynamic heat and mass transfer from a stretching surface to a saturated porous medium with Soret and Dufour effects. *Comp Mater Sci.* 2009;46(1):57-65.
17. Ali MM, Mamun AA, Maleque MA, Azim NHMA. Radiation effects on MHD free convection flow along vertical flat plate in presence of Joule heating and heat generation. *Procedia Eng.* 2013;56:503-9.
18. Nayak MK, Dash GC, Singh LP. Unsteady radiative MHD free convective flow and mass transfer of a viscoelastic fluid past an inclined porous plate. *Arab J Sci Eng.* 2015;40(11):3029-39.
19. Mburu ZM. Hydromagnetic Fluid Flow between Parallel Plates where the Upper Plate is Porous in Presence of Variable Transverse Magnetic Fields (Doctoral dissertation, MSC Applied Mathematics, JKUAT); 2016.
20. Umamaheswar M, Varma SVK, Raju MC, Chamkha AJ. Unsteady magnetohydrodynamic free convective double-diffusive viscoelastic fluid flow past an inclined permeable plate in the presence of viscous dissipation and heat absorption. *Special Topics Rev Porous Media.* 2015;6(4):333-42.
21. Hayat T, Khan MI, Tamoor M, Waqas M, Alsaedi A. Numerical simulation of heat transfer in MHD stagnation point flow of Cross fluid model towards a stretched surface. *Results Phys.* 2017;7:1824-7.
22. Hamad MAA, Pop I, Md Ismail AI. Magnetic field effects on free convection flow of a nanofluid past a vertical semi-infinite flat plate. *Nonlinear Anal Real World Appl.* 2011;12(3):1338-46.
23. Reddy GR, Murthy CVR, Reddy NB. MHD flow over a vertical moving porous plate with heat generation by considering double diffusive convection. *Int J Appl Math Mech.* 2011;7(1):1-17.
24. Makinde OD, Khan WA, Khan ZH. Buoyancy effects on MHD stagnation point flow and heat transfer of a nanofluid past a convectively heated stretching/shrinking sheet. *Int J Heat Mass Transf.* 2013;62:526-33.
25. Ali B, Ahammad NA, Windarto, Oke AS, Shah NA, Chung JD, J. D. Significance of tiny particles of dust and TiO₂ subject to Lorentz force: The case of non-newtonian dusty rotating fluid. *Mathematics.* 2023; 11(4):877.
26. Oke AS. Coriolis effects on MHD flow of MEP fluid over a non-uniform surface in the presence of thermal radiation. *Int Commun Heat Mass Transf.* 2021;129:105695.
27. Koriko OK, Adegbe KS, Oke AS, Animasaun IL. Exploration of Coriolis force on motion of air over the upper horizontal surface of a paraboloid of revolution. *Phys Scr.* 2020;95(3):035210.
28. Koriko OK, Adegbe KS, Oke AS, Animasaun IL. Corrigendum: exploration of Coriolis force on motion of air over the upper horizontal surface of a paraboloid of revolution. *Phys Scr. Phys. Scr.* 2020;95:95(11), 119501: 035210.
29. Animasaun IL, Oke AS, Al-Mdallal QM, Zidan AM. Exploration of water conveying carbon nanotubes, graphene, and copper nanoparticles on impermeable stagnant and moveable walls experiencing variable temperature: thermal analysis. *J Therm Anal Calorim.* 2023;148(10):4513-22.
30. Oke AS, Eyinla T, Juma BA. Effect of Coriolis force on Modified Eyring Powell Fluid flow. *J Eng Res Rep.* 2023;24(4):26-34.
31. Oke AS. Combined effects of Coriolis force and nanoparticle properties on the dynamics of gold-water nanofluid across nonuniform surface. *ZAMM-journal of applied mathematics and mechanics. Z Angew Math Mech.* 2022;102(9):e202100113.
32. Xing JT. Fluid-Solid interaction dynamics: theory, variational principles, numerical methods, and applications. Academic Press; 2019.

© 2023 Onyinkwa and Chepkwony; This is an Open Access article distributed under the terms of the Creative Commons Attribution License (<http://creativecommons.org/licenses/by/4.0>), which permits unrestricted use, distribution, and reproduction in any medium, provided the original work is properly cited.

Peer-review history:

The peer review history for this paper can be accessed here:
<https://www.sdiarticle5.com/review-history/102081>